Chemical Science

www.rsc.org/chemicalscience

Volume 4 | Number 2 | February 2013 | Pages 541–864

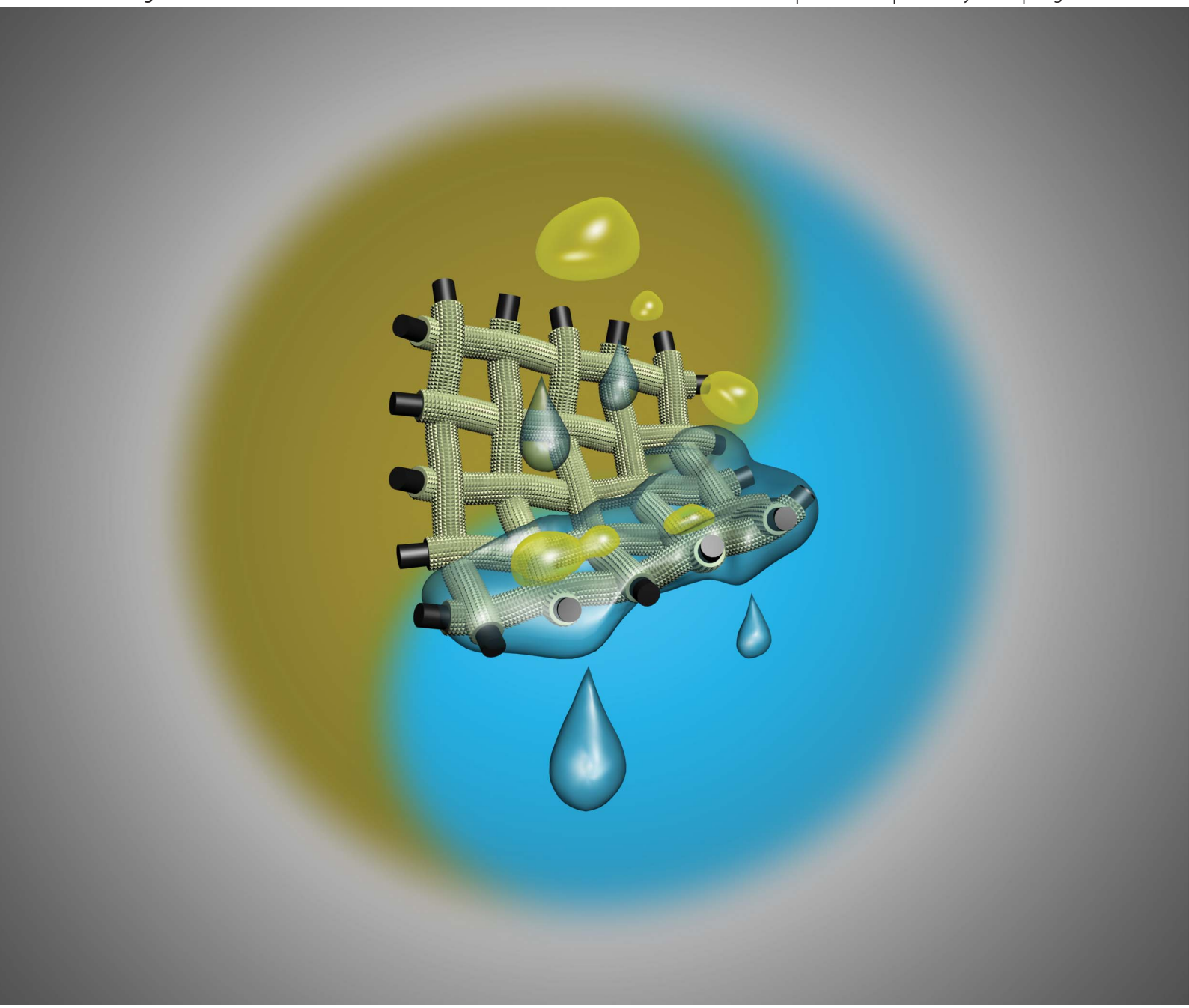

ISSN 2041-6520

RSC Publishing

EDGE ARTICLE

Jihong Yu *et al.*

Zeolite-coated mesh film for efficient oil–water separation

Chemical Science

RSC Publishing

EDGE ARTICLE

View Article Online
View Journal | View Issue

Cite this: *Chem. Sci.*, 2013, **4**, 591

Zeolite-coated mesh film for efficient oil–water separation†

Qiang Wen,‡[a] Jiancheng Di,‡[a] Lei Jiang,[b] Jihong Yu*[a] and Ruren Xu[a]

Oil–water separations are helping with urgent issues due to increasing industrial oily wastewater, as well as frequent oil spill accidents. Membrane-based materials with special wettability are desired to separate oils from water. However, fabrication of energy-efficient and stable membranes that are suitable for practical oil–water separation remains challenging. Zeolite films have attracted intense research interest due to their unique pore character, excellent chemical, thermal and mechanical stability, *etc.* Here we first demonstrate zeolite-coated mesh films for gravity-driven oil–water separation. High separation efficiency of various oils can be achieved based on the excellent superhydrophilicity and underwater superoleophobicity of the zeolite surface. Flux and intrusion pressure are tunable by simply changing the pore size, dependent on the crystallization time of the zeolite crystals, of the zeolite meshes. More importantly, such films are corrosion-resistant in the presence of corrosive media, which gives them promise as candidates in practical applications of oil–water separation.

Received 17th October 2012
Accepted 22nd November 2012

DOI: 10.1039/c2sc21772d

www.rsc.org/chemicalscience

Introduction

Oil–water separation has become an increasingly important and urgent issue in modern chemical industrial process and environmental protection due to increasing industrial oily wastewater, as well as frequent oil spill accidents. Many materials have been developed for oil–water separation by utilizing their special wettability. For example, some "oil-removing" type of materials, with both hydrophobic and oleophilic properties have been used to absorb oil from water,[1] such as kapok,[2,3] activated carbon,[4,5] hydrophobic aerogels,[6–9] crosslinked polymers,[10,11] *etc.* However, such materials suffer from the limitation of recyclability and secondary pollution during the post-treatment process as well as a waste of both absorbed oil and oleophilic materials. Therefore, membrane-based technologies are attractive for the separation of oil and water, and some superhydrophobic and superoleophilic membranes have been successfully fabricated.[12–20] However, it is energy-intensive to use these membranes because water tends to form a barrier layer between the oil and the hydrophobic surface during the separation process owing to its higher density, thus preventing the permeation of oil. Recently, the oil-repellent ability of fish scales in aqueous media has attracted increasing interest[21] and a series of materials with performance similar to fish scales have been adopted for the separation of oil and water, such as hydrogels,[22] pH-responsive polymers,[23] and hydro-responsive polymers.[24] However, such organic layers are unstable when exposed to some harsh conditions. Therefore, there is a great need to design stable inorganic films for practical applications in oil–water separation.

Zeolites with regular nanoporous structures are crystalline oxide solids that are widely used in the fields of catalysis, adsorption and ion exchange.[25,26] Because of the characteristics of high selectivity and low energy consumption, considerable progress in separations by utilizing continuous zeolite membranes or films has been achieved in the past decades.[27–31] Particularly, high-silica and pure-silica zeolite coatings have been demonstrated to be corrosion-resistant owing to the extraordinary thermal, mechanical and chemical stability.[32–34] In addition, the hydrophilicity and tunable density of charged groups on the film surface facilitate zeolite coatings to be good candidates with applications as anti-biofouling surfaces.[35,36]

Here we demonstrate a novel oil–water separation film prepared by growing pure-silica zeolite silicalite-1 (MFI type) crystals on stainless steel mesh by taking advantage of the wettability and stability of zeolite film. The zeolite-coated mesh films (ZCMFs) show outstanding superhydrophilic and underwater superoleophobic properties. The separation methodology is solely based on gravity, which allows water to permeate through the film quickly, whereas the oil phase is retained above the film, thus proving to be an energy-efficient filter for oil–water separation. Meanwhile, the underwater

[a]*State Key Laboratory of Inorganic Synthesis and Preparative Chemistry, Jilin University, Qianjin Street 2699, Changchun 130012, P.R. China. E-mail: jihong@jlu.edu.cn; Fax: +86-431-8516-8608; Tel: +86-431-8516-8608*

[b]*School of Chemistry and Environment, Beihang University, Beijing 100191, P.R. China*

† Electronic supplementary information (ESI) available: Detailed materials, characterization and measurements; curve of pore diameters of ZCMFs changed with the crystallization time; XRD pattern of ZCMF-12; SEM image and XRD pattern of ZCMF-12 after corrosion test; video of the separation process. See DOI: 10.1039/c2sc21772d

‡ These authors contributed equally.

superoleophobic interface with low affinity for oil drops prevents the film from fouling by oils, and the trace amount of oil can be simply removed by calcination. More importantly, such films are highly stable under various harsh conditions, such as acid and concentrated salt, *etc.* Our work shows that ZCMFs are suitable for future practical applications in oil–water separation.

Experimental section

Preparation of silicalite-1 crystal seeds

Silicalite-1 crystal seeds were prepared from a clear solution with a molar ratio of tetra-*n*-propylammonium hydroxide (TPAOH) : tetraethylorthosilicate (TEOS) : H_2O : EtOH = 9 : 25 : 480 : 100. The reaction solution was sealed in a 50 mL polypropylene bottle and conducted at 90 °C for 4 days according to the literature.[37] The product was purified by repeated centrifugation until the pH value was close to 7 and then dried in the oven overnight (60 °C).

Seeding process and secondary growth

An aqueous solution of seeds (20 g L^{-1}) was prepared by dispersing the silicalite-1 crystal seeds into water and the pH value was adjusted to 10 with ammonia. Then pre-cleaned stainless steel mesh (360 mesh, 3.5 × 3.5 cm) was immersed into the seed solution for 15 min under ultrasonic vibration conditions and dried in the oven for 2 hours (120 °C). The seeded mesh was placed vertically in a 100 mL Teflon-lined stainless steel autoclave and immersed into 60 g reaction solution with a molar ratio of KOH : tetra-*n*-propylammonium bromide (TPABr) : H_2O : TEOS : EtOH = 1 : 1 : 1000 : 4.4 : 15.6. After secondary crystallization at 175 °C for *x* h (*x* from 2 to 16), ZCMFs were obtained and named as ZCMF-*x*.

Oil–water separation experiments of the ZCMFs

The as-prepared ZCMF was fixed between two Teflon flanges, a mixture of water and oil (50% v/v) was poured onto the film through a glass tube, the permeated liquid was collected in a jar. The driving force during the separation process is its own gravity.

Results and discussion

Synthesis of ZCMFs

The ZCMFs were prepared through a seeding and secondary growth process under hydrothermal conditions. Fig. 1a shows the scanning electron microscope (SEM) image of the bare stainless steel mesh with pore size around 42 μm, and the inset exhibits zeolite seeds around 150 nm in size, which were dispersed uniformly on the stainless steel wires. An image of zeolite-coated mesh film after secondary growth for 12 h (ZCMF-12) is shown in Fig. 1b. It can be seen that the original mesh has been completely covered by zeolite crystals and the pore size of the mesh decreases obviously. The magnified image (Fig. 1c) shows the micro/nanoscale hierarchical rough surface of as-prepared zeolite mesh film. A classic cross-section (Fig. 1d)

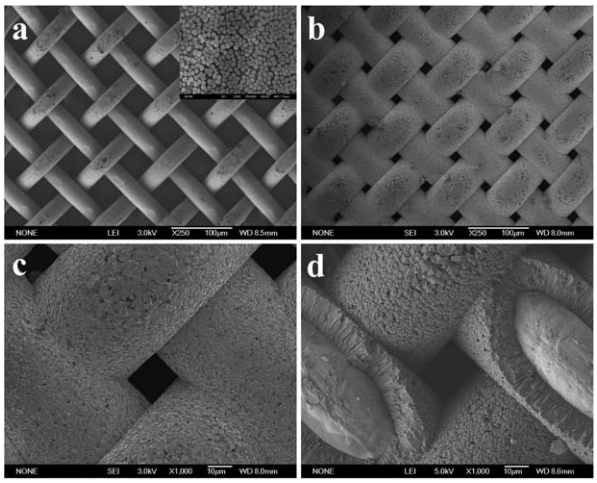

Fig. 1 SEM images of ZCMF-12 prepared by seeding and secondary growth process. (a) Large scale view of the bare stainless steel mesh with an average pore diameter of about 42 μm, the inset is the magnified image of the mesh after seeding process. (b) Large scale image of ZCMF-12. (c) Magnified view of a single pore, and its (d) cross-sectional view.

reveals that the silicalite-1 crystals are closely attached to the substrate, and are oriented with their *c*-axes perpendicular to the stainless steel wire. The pore size of ZCMFs can be systematically modulated by simply changing the crystallization time. As shown in Fig. S1 (see ESI†), the pore size of the meshes decreases almost linearly with the growth of zeolite crystals. Eventually, a continuous zeolite film can be obtained when the crystallization time reaches over 20 h. The X-ray diffraction (XRD) pattern of ZCMF-12 in Fig. S2† fits well with the simulated XRD pattern of the MFI structure, indicating that the zeolite phase in the film is highly crystalline silicalite-1.

Wettability study of ZCMFs

As is well-known, the wettability of solid surfaces strongly depends on both the chemical composition and the geometrical structure.[38] Herein, we take ZCMF after crystallization for 12 h (ZCMF-12) as representative to characterize the property of wettability. ZCMF-12 is superamphiphilic in an air–solid–liquid three-phase system with both the water contact angle (CA) and the oil contact angle (OCA) lower than 10° (Fig. 2a and b). This originates from the micro/nanoscale hierarchical surface (Fig. 1c) and the existence of massive Si–OH groups on the surface of silicalite-1 crystals. When pre-wetted in aqueous media, ZCMF-12 becomes highly oil-repulsive for various oils, such as petroleum ether, cyclohexane, soybean oil, diesel and crude oil. Fig. 2c (black column) shows the underwater OCAs for a selection of oils, and the typical photographs of oil droplets on the mesh film surface are shown as the insets. All of the OCAs are above 150°, suggesting that ZCMF-12 possesses extraordinary underwater superoleophobic properties. This phenomenon is attributed to the formation of a water cushion between the oil droplet and the solid surface composed of trapped water molecules in the interspaces of the rough surface, which offers a strong repulsive force due to the repulsive

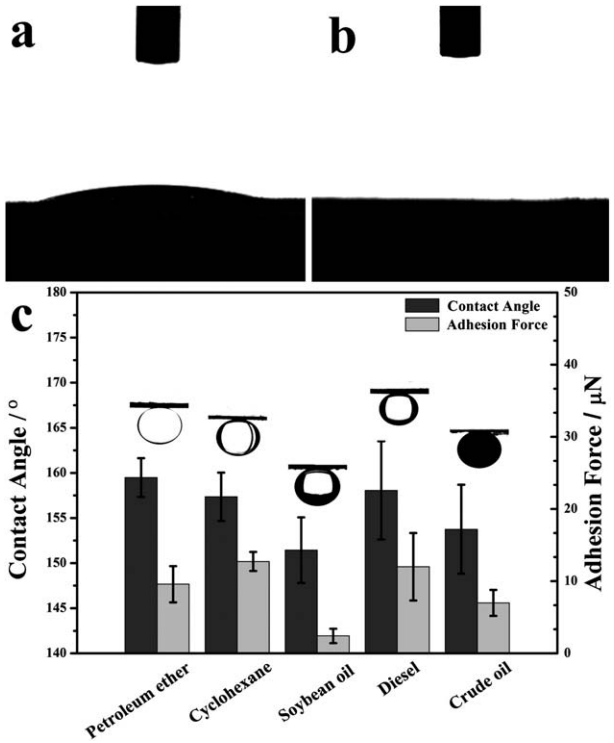

Fig. 2 Special wettability of ZCMF-12. Photographs of (a) water droplet (5 μL) and (b) oil droplet (1,2-dichloroethane, 5 μL) on ZCMF-12 in air. (c) The underwater superoleophobic and low oil-adhesion characteristics of ZCMF-12 in oil–water–solid three-phase system. All the OCAs (c, black column) in water of ZCMF-12 for a selection of oils are above 150°, and the oil-adhesion forces (c, gray column) are below 13 μN. The insets are representative photographs of oil droplet (2 μL) on ZCMF-12 in water.

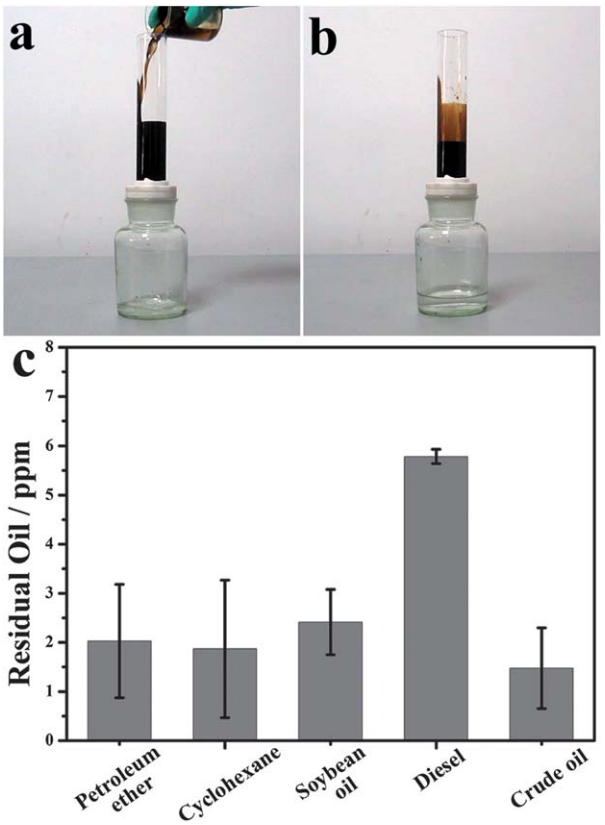

Fig. 3 Oil–water separation studies of ZCMF-12. (a) ZCMF-12 was fixed between two Teflon flanges, and the crude oil–water mixture was poured into the top glass tube. (b) Water selectively permeated through ZCMF-12, while the crude oil was intercepted and kept in the upper tube. (c) The residual oil content in the collected water for a selection of oils.

interaction between polar (water) and non-polar (oil) molecules.[22,23] The trapped aqueous layer also contributes to decrease the oil-adhesion force. As shown in Fig. 2c (gray column), the adhesion forces of different oils are all less than 13 μN. Such low adhesion properties can prevent the ZCMFs from fouling by oil during the separation process.

Separation of oil and water

The separation of oil and water was carried out by using the setup as illustrated in Fig. 3a. A mixture of crude oil and water (50%, v/v) was poured onto the water pre-wetted ZCMF-12 that was fixed between two Teflon flanges and the only driving force was on its own gravity. Water with higher density than oil permeated through the film quickly, and no visible oil was observed in the collected water (Fig. 3b). A video illustrating the separation of crude oil and water is provided as ESI, Movie S1.†

To further study the separation efficiency, the residual oil content in water was measured. Experimental results in Fig. 3c show that there exists only a trace amount of oil in water, *i.e.*, less than 6 ppm, which reveals that the mixtures of water and oil could be separated effectively by ZCMF-12.

Water flux and intrusion pressure of cyclohexane were also introduced to testify the separation efficiency of ZCMFs. The water flux (F) was measured under a fixed column of water. The values were calculated using eqn (1):

$$F = V/St \quad (1)$$

where V is the volume of water that permeates through the membrane, here we fixed V to 1 L, S is the area of the membrane, and t is the required time for the permeation of 1 L water. The intrusion pressure (P) values were calculated using eqn (2):

$$P = \rho g h_{\max} \quad (2)$$

where ρ is the density of cyclohexane, g is acceleration of gravity, and $h_{\max}$ is the maximum height of cyclohexane that the ZCMFs can support. Fig. 4 shows the influence of pore sizes of ZCMFs on water flux and intrusion pressure of cyclohexane. The water flux increases with the increase of the pore size of ZCMFs, but it is inversed to the intrusion pressure of oil. It can be explained that larger pore size of ZCMFs is more favourable for the permeation of water, meanwhile leads to the reduction of the thickness of the trapped aqueous layer, which can not offer enough surface tension to support too much oil. When the pore size of ZCMF-16 decreases to 5 μm, water hardly passes through the membrane, on the contrary, ZCMF-2 will lose selectivity for oil and water when the pore size goes beyond 41 μm. Herein, ZCMF-12 represents the optimal pore size of around 14 μm,

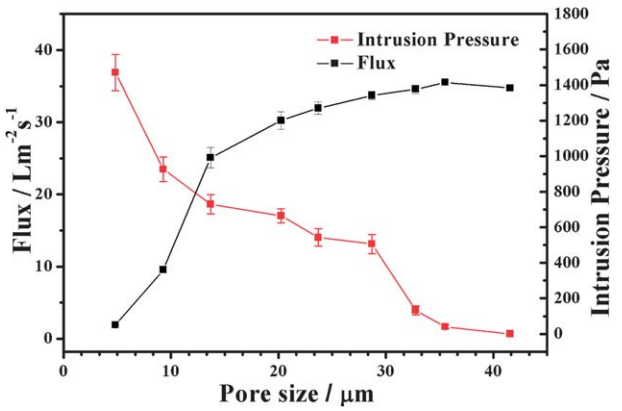

Fig. 4 Influence of pore sizes of ZCMFs on water flux and intrusion pressure of cyclohexane. Black line: water flux, red line: intrusion pressure of cyclohexane.

giving rise to the water flux as high as 25 L m^{-2} s^{-1} and the intrusion pressure of 729 Pa.

Stability and recyclability

The anti-corrosion performance of ZCMF-12 was studied by immersing the film into corrosive medium of 0.1 M HCl for 48 h and 1 M NaCl for 1 month, respectively. Fig. S3† shows the SEM image and XRD pattern of ZCMF-12 after the corrosion test. Neither micro/nanoscale hierarchical structure of the solid surface nor the MFI framework of zeolites was destroyed by the corrosive solution. Moreover, no change on the separation efficiency in crude oil–water system was observed compared with the fresh-prepared ZCMF-12, proving that the ZCMFs had good stability in harsh condition. Recyclability of ZCMFs was further investigated by repeating the separation process. Samples retain the superoleophobicity and low oil-adhesion properties after 10 uses, showing a stable performance on oil–water separation. In addition, ZCMFs can also be regenerated by calcination owing to the high thermal stability of zeolite crystals.

Conclusions

In summary, we have developed a facile and straightforward way to fabricate zeolite-coated mesh films (ZCMFs) with superhydrophilicity and underwater superoleophobicity. Various oils can be efficiently separated from water based on the gravity-driven separation process. Such films with low oil-adhesion properties are easily recyclable and residual trace oils can be simply removed by calcination while do not change the wettability of the films. The anti-corrosion behaviour confirms that the ZCMFs are highly stable in the harsh environments, which makes them an ideal candidate for applications in industry and everyday life, such as the oil retention barrier of industrial outlet sewer pipes, oil fences for oil spill accidents, separation of living waste oil, *etc.* Furthermore, multi-functional devices with smart surface could be designed that may possess performances of ion exchange, catalysis and separation simultaneously by combining the inherent structural characteristics of zeolites as well as their special wettability.

Acknowledgements

The present work was supported by the State Basic Research Project of China (Grant no. 2011CB808703) and the National Natural Science Foundation of China.

Notes and references

1 M. O. Adebajo, R. L. Frost, J. T. Kloprogge, O. Carmody and S. Kokot, *J. Porous Mater.*, 2003, **10**, 159–170.
2 X. Huang and T.-T. Lim, *Desalination*, 2006, **190**, 295–307.
3 T.-T. Lim and X. Huang, *Ind. Crops Prod.*, 2007, **26**, 125–134.
4 Z. Yue and J. Economy, *J. Nanopart. Res.*, 2005, **7**, 477–487.
5 M. Razvigorova, T. Budinova, N. Petrov and V. Minkova, *Wat. Res.*, 1998, **32**, 2135–2139.
6 J. T. Korhonen, M. Kettunen, R. H. A. Ras and O. Ikkala, *ACS Appl. Mater. Interfaces*, 2011, **3**, 1813–1816.
7 A. Venkateswara Rao, N. D. Hegde and H. Hirashima, *J. Colloid Interface Sci.*, 2007, **305**, 124–132.
8 J. G. Reynolds, P. R. Coronado and L. W. Hrubesh, *J. Non-Cryst. Solids*, 2001, **292**, 127–137.
9 L. W. Hrubesh, P. R. Coronado and J. H. Satcher, *J. Non-Cryst. Solids*, 2001, **285**, 328–332.
10 E. Baruch-Teblum, Y. Mastai and K. Landfester, *Eur. Polym. J.*, 2010, **46**, 1671–1678.
11 Y. Zhang, S. Wei, F. Liu, Y. Du, S. Liu, Y. Ji, T. Yokoi, T. Tatsumi and F. Xiao, *Nano Today*, 2009, **4**, 135–142.
12 L. Feng, Z. Zhang, Z. Mai, Y. Ma, B. Liu, L. Jiang and D. Zhu, *Angew. Chem., Int. Ed.*, 2004, **43**, 2012–2014.
13 X. Chen, L. Hong, Y. Xu and Z. W. Ong, *ACS Appl. Mater. Interfaces*, 2012, **4**, 1909–1918.
14 C. Wang, T. Yao, J. Wu, C. Ma, Z. Fan, Z. Wang, Y. Cheng, Q. Lin and B. Yang, *ACS Appl. Mater. Interfaces*, 2009, **1**, 2613–2617.
15 Q. Pan, M. Wang and H. Wang, *Appl. Surf. Sci.*, 2008, **254**, 6002–6006.
16 C. Lee and S. Baik, *Carbon*, 2010, **48**, 2192–2197.
17 F. Qin, Z. Yu, X. Fang, X. Liu and X. Sun, *Front. Chem. Sci. Eng.*, 2009, **3**, 112–118.
18 D. Tian, X. Zhang, X. Wang, J. Zhai and L. Jiang, *Phys. Chem. Chem. Phys.*, 2011, **13**, 14606–14610.
19 J. Kong and K. Li, *Sep. Purif. Technol.*, 1999, **16**, 83–93.
20 J. Yang, Z. Zhang, X. Xu, X. Zhu, X. Men and X. Zhou, *J. Mater. Chem.*, 2012, **22**, 2834–2837.
21 M. Liu, S. Wang, Z. Wei, Y. Song and L. Jiang, *Adv. Mater.*, 2009, **21**, 665–669.
22 Z. Xue, S. Wang, L. Lin, L. Chen, M. Liu, L. Feng and L. Jiang, *Adv. Mater.*, 2011, **23**, 4270–4273.
23 L. Zhang, Z. Zhang and P. Wang, *NPG Asia Mater.*, 2012, **4**, DOI: 10.1038/am.2012.1014.
24 A. K. Kota, G. Kwon, W. Choi, J. M. Mabry and A. Tuteja, *Nat. Commun.*, 2012, **3**, DOI: 10.1038/ncomms2027.
25 F. Schüth and W. Schmidt, *Adv. Mater.*, 2002, **14**, 629–638.

26 A. Corma, *Chem. Rev.*, 1997, **97**, 2373–2419.
27 M. A. Snyder and M. Tsapatsis, *Angew. Chem., Int. Ed.*, 2007, **46**, 7560–7573.
28 J. Caro and M. Noack, *Microporous Mesoporous Mater.*, 2008, **115**, 215–233.
29 E. E. McLeary, J. C. Jansen and F. Kapteijn, *Microporous Mesoporous Mater.*, 2006, **90**, 198–220.
30 S. R. Chowdhury, J. De Lamare and V. Valtchev, *J. Membr. Sci.*, 2008, **314**, 200–205.
31 X. Zou, P. Bazin, F. Zhang, G. Zhu, V. Valtchev and S. Mintova, *ChemPlusChem*, 2012, **77**, 437–444.
32 R. S. Bedi, L. P. Zanello and Y. Yan, *Adv. Funct. Mater.*, 2009, **19**, 3856–3861.
33 R. Cai, M. Sun, Z. Chen, R. Munoz, C. O'Neill, D. E. Beving and Y. Yan, *Angew. Chem., Int. Ed.*, 2008, **47**, 525–528.
34 C. M. Lew, R. Cai and Y. Yan, *Acc. Chem. Res.*, 2010, **43**, 210–219.
35 A. Damayanti, Z. Ujang and M. R. Salim, *Bioresour. Technol.*, 2011, **102**, 4341–4346.
36 G. Chen, D. E. Beving, R. S. Bedi, Y. S. Yan and S. L. Walker, *Langmuir*, 2009, **25**, 1620–1626.
37 J. Di, H. Chen, X. Wang, Y. Zhao, L. Jiang, J. Yu and R. Xu, *Chem. Mater.*, 2008, **20**, 3543–3545.
38 T. Sun, L. Feng, X. Gao and L. Jiang, *Acc. Chem. Res.*, 2005, **38**, 644–652.